Mechanism of the Hydrosilylation Reaction of Alkenes at Porous Silicon: Experimental and Computational Deuterium Labeling Studies

Louis C. P. M. de Smet,[†] Han Zuilhof,*[,†] Ernst J. R. Sudhölter,[†] Lars H. Lie,[‡] Andrew Houlton,[‡] and Benjamin R. Horrocks*[,‡]

Laboratory of Organic Chemistry, Wageningen University, Dreijenplein 8, 6703 HB Wageningen, The Netherlands, and School of Natural Sciences, Bedson Building, University of Newcastle upon Tyne, Newcastle upon Tyne NE1 7RU, U.K.

Received: December 9, 2004; In Final Form: February 18, 2005

The mechanism of the formation of Si−C bonded monolayers on silicon by reaction of 1-alkenes with hydrogen-terminated porous silicon surfaces has been studied by both experimental and computational means. We propose that monolayer formation occurs via the same radical chain process as at single-crystal surfaces:[1] a silyl radical attacks the 1-alkene to form both the Si−C bond and a radical center on the β-carbon atom. This carbon radical may then abstract a hydrogen atom from a neighboring Si−H bond to propagate the chain. Highly deuterated porous silicon and FTIR spectroscopy were used to provide evidence for this mechanism by identifying the IR bands associated with the C−D bond formed in the proposed propagation step. Deuterated porous silicon surfaces formed by galvanostatic etching in 48% DF/D_2O:EtOD (1:1) electrolytes showed a 30% greater density of Si−D sites on the surface than Si−H sites on hydrogen-terminated porous silicon surfaces prepared in the equivalent H-electrolyte. The thermal reaction of undec-1-ene and the Lewis acid catalyzed reaction of styrene on a deuterated surface both resulted in alkylated surfaces with the same C−C and C−H vibrational features as formed in the corresponding reactions at a hydrogen-terminated surface. However, a broad band around 2100 cm^{-1} was observed upon alkylating the deuterated surfaces. Ab initio and density functional theory calculations on small molecule models showed that the integrated absorbance of this band was comparable to the intensity expected for the C−D stretches predicted by the chain mechanism. The calculations also indicate that there is substantial interaction between the hydrogen atoms on the β-carbons and the hydrogen atoms on the Si(111)−H surface. These broad 2100 cm^{-1} features are therefore assigned to C−D bands arising from the involvement of surface D atoms in the hydrosilylation reactions, while the line broadening can be explained partly by interaction with neighboring surface atoms/groups.

Introduction

A variety of methods for the formation of robust, Si−C bonded monolayers at hydrogen-terminated silicon surfaces have been reported.[1−23] The reaction of 1-alkenes with the hydrogen-terminated silicon surface is a flexible reaction, since monolayers can be formed by photochemical[9,10,19,21−23] or thermal[1,5,24,25] means or by employing catalysts ($EtAlCl_2$ or H_2PtCl_6) on porous silicon and single-crystal surfaces.[3,12,26] The surface modification has also been explored for 1-alkynes.[27,28] In many cases little or no oxidation of the silicon sample occurs in parallel with the monolayer formation.[29] Si−C bonded organic monolayers formed from the reaction of 1-alkenes or 1-alkynes with hydrogen-terminated surfaces have attracted considerable interest due to their stability and structural order.[1,3,28,30−32] These monolayers have been used as a platform for several immobilization chemistries, e.g., DNA,[33−35] polymer grafting,[36] further organic reactions,[7,32] or solid-phase oligosynthesis.[37−39] They have also been used to cap silicon nanoparticles.[39,40]

The structure of monolayers formed on silicon by hydrosilylation of 1-alkenes and 1-alkynes has been studied by polarized FTIR and contact angle experiments, X-ray analysis,[1,17,27] impedance spectroscopy,[41−43] and a variety of theoretical techniques including molecular mechanics,[44] molecular dynamics,[45] and density functional computations.[44,46−51] The monolayers show a substantial degree of ordering, and an approximately all-trans conformation of the alkyl chains with a well-defined tilt angle between the surface normal and the alkyl chains of ca. 30° is observed.[1,32,44] Polarized visible-IR sum frequency spectra provide evidence that the monolayer forms epitaxially on Si(111) substrates with some solidlike order but significant numbers of gauche defects.[52−54] The presence of CH_2 features in these sum-frequency spectra was consistent with the computational studies,[44,45] which suggest the torsional angles at the base of the alkyl chain deviate from the values for the ideal all-trans conformation—a "twisted stem" model.[52] Since the Si−C and Si−Si bonds are covalent and rather inert, the ordering cannot be explained as the result of an annealing process like that which is believed to operate in thiol-based self-assembled monolayers (SAMs) on gold surfaces.[55] The mechanism of the monolayer-forming reaction of 1-alkenes with hydrogen-terminated silicon is therefore critical to the understanding of the physicochemical properties of the monolayers. Linford et al.[1] suggested a radical chain mechanism in which a silyl radical attacks the 1-alkene to form the Si−C bond, and a radical center on the β-carbon atom is formed. This kinetic chain prop-

* Corresponding author. (B.R.H.) Telephone: +44-191-222-5619. FAX: +44-191-222-6929. E-mail: b.r.horrocks@ncl.ac.uk. (H.Z.) Telephone: +31-317-482367. FAX: +31-317-484914. E-mail: han.zuilhof@wur.nl.

[†] Wageningen University.

[‡] University of Newcastle upon Tyne.

10.1021/jp044400a CCC: $30.25
Published on Web 05/27/2005

SCHEME 1: Proposed Reaction Scheme for the Formation of Alkyl Monolayers on H-Terminated Silicon by a Thermal Hydrosilylation Reaction[a]

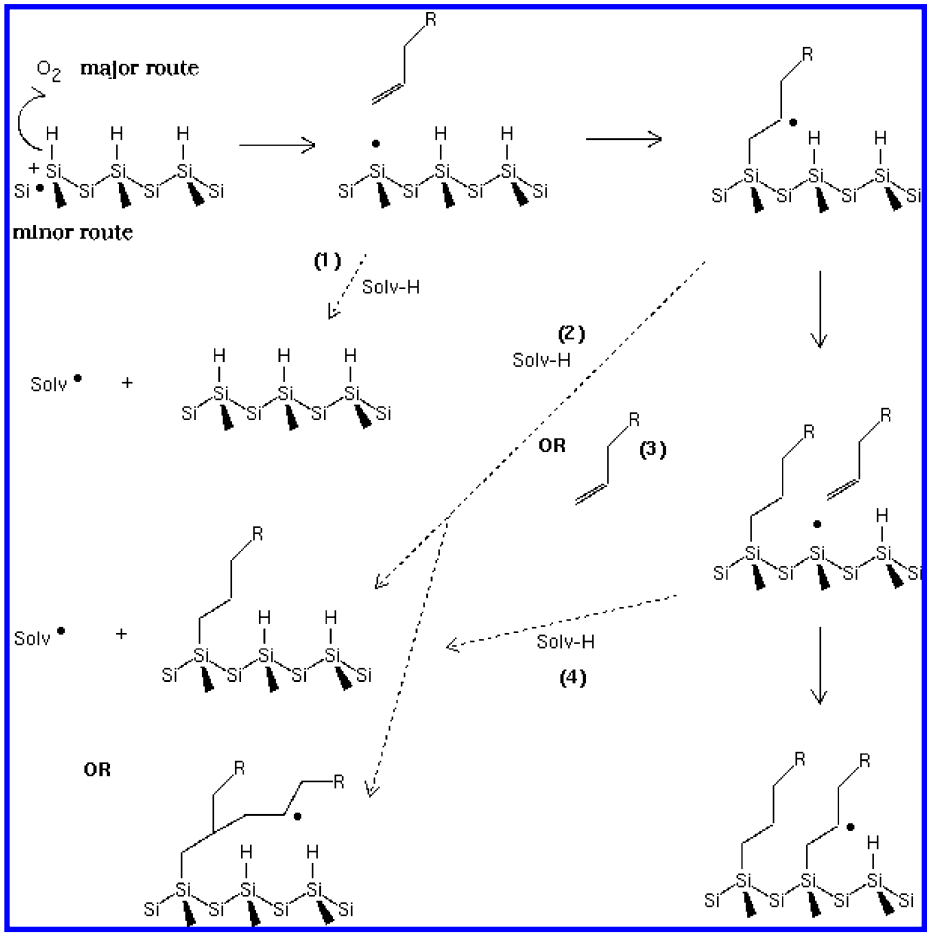

[a] The scheme commences in the top left corner of the diagram with a radical initiation step, which is either abstraction of a hydrogen atom, e.g., by trace oxygen, or another reaction involving the majority carriers (holes) followed by loss of a proton. The extent to which each process actually occurs is discussed in the text; the major pathway is indicated by the solid arrows showing the propagation of the radical chain and the formation of the monolayer. The dashed arrows indicate the various plausible side reactions we consider and are numbered 1−4.

agates by abstraction of an H atom from the nearest-neighbor Si atom by the carbon-centered radical, as shown in Scheme 1.

According to such a mechanism the monolayer grows by addition of 1-alkenes to the end of a kinetic chain, which walks across the surface, rather than stepwise at random individual Si sites. Some direct evidence for this mechanism has been provided for Si(100)−H surfaces in ultrahigh vacuum on which monolayers formed from styrene were observed to propagate along rows of silicon atoms starting from individual dangling bonds.[56] More recently, the reaction of styrene with the Si(111)−H face has been studied and islands containing on the order of 20 phenyl rings were formed at the sites of single dangling bonds,[57,58] while also the visible-light induced wet-chemical attachment reaction of 1-decene[21,22] proceeds via the formation of islands.[59] Several open questions remain, since it is not clear in general what conditions are required for this to happen. For example, propene molecules did not show the behavior displayed by styrene.[56] There is also a question as to whether the growing chain generates a structure determined by a self-avoiding random walk[9] or, as may occur in the case of styrene/Si(111)−H, some attractive interaction between the molecules leads to the formation of islands.[57,60] Further, there is comparatively little information on whether the same mechanism operates in the hydrosilylation of porous silicon, where direct observation by scanning tunneling microscopy (STM) is unlikely to be possible.

Some attempts to test the mechanism by deuterium labeling experiments and FTIR have also been made.[61,62] The essence of these experiments is to follow the fate of the H (or D) atoms on the surface as the reaction proceeds, since the radical chain mechanism (Scheme 1) predicts that the surface H atoms become incorporated into the monolayer at the β-carbons of the alkyl chains. Using styrene- d_8, Stewart and Buriak reported the observation of C−H stretches in transmission FTIR upon reaction with hydrogen-terminated porous silicon samples.[61] Since a different behavior of propene compared to styrene has been observed on single-crystal Si(100)−H by ultrahigh-vacuum STM,[56] the reaction of straight-chain 1-alkenes on porous silicon is of interest because such molecules are very frequently employed for surface modifications. We have previously studied the reaction of undec-1-ene from dilute (0.1 M) toluene solution on deuterated, abraded silicon crystals by transmission FTIR and found no evidence for incorporation of deuterium as would be indicated by the radical chain mechanism.[62] Wolkow and Wayner have suggested that this result can also be interpreted as a primary kinetic isotope effect on the abstraction of D atoms and that the C−D signals may be too weak to detect.[20] In previous work we were not able to study porous silicon, since the observation of C−D bonds was complicated by the overlap of residual Si−H bands with the C−D stretches. However, in this report, we have prepared and characterized highly deuterated porous silicon surfaces, which have a higher surface area than

abraded silicon and allow us to analyze the intensity of the features in the 2100 cm^{-1} region. Using such highly deuterated surfaces, we are able to demonstrate the presence of C−D stretching bands in the monolayer, which supports the proposed radical chain mechanism on porous silicon under thermal reflux of undec-1-ene from both toluene and benzene solutions. The evidence for the presence of C−D bonds comes from the enhancement in the intensity in the 2100 cm^{-1} region and a theoretical analysis of the factors determining the intensity and broadening of the peaks observed in this region. We also compare the results from the room-temperature Lewis acid ($EtAlCl_2$) catalyzed reactions of undec-1-ene, which would be expected to occur via a mechanism similar to that of hydrosilylation in molecular chemistry.[63]

Experimental Section

Materials. All common reagents were obtained from Sigma-Aldrich at 99% purity. Benzene, predried over sodium wires, was dried in a potassium-coated Schlenk flask or over molecular sieve beads (type 3 Å from Sigma-Aldrich). Toluene was freshly distilled (over Na) before use. Benzene-d_6 (99.96 at. % D, Sigma-Aldrich) and EtOD (C_2H_5OD, 99 at. % D, GOSS Scientific Instrument, Ltd., Essex, U.K.) were dried over molecular sieves before use. D_2O (99.9 at. % D, Cambridge Isotope Laboratories, Andover, MA), 48% (w/w) HF in H_2O (Fluka), toluene-d_8 (99.94 at. % D, Cambridge Isotope), $EtAlCl_2$ (1.0 M in hexanes, Sigma-Aldrich), and styrene (99+%, Sigma-Aldrich) were all used as received.

In a sealed plastic system, 40% (w/w) DF in D_2O (Fluorochem Ltd., Derbyshire, U.K.; custom preparation with no atom percent D specified by manufacturer) was stored under a blanket of dry nitrogen (from boil-off of the local liquid N_2 storage facility). Samples were transferred by syringe and used immediately for preparation of deuterated porous silicon.

Porous Silicon. Silicon wafers (⟨100⟩ oriented; boron-doped, *p*-type, 10 Ω cm resistivity, Compart Technology, Cambridge, U.K.) were degreased in acetone before production of a clean oxide layer by immersion in freshly prepared "piranha" solution (1:1 (v/v) concentrated H_2SO_4 and 30% H_2O_2) for 10 min at room temperature. Hydrogen-terminated porous silicon (PS−H) was formed by galvanostatic anodization of a cleaned, freshly oxidized, boron-doped *p*-Si(100) wafer. The oxide was removed from one side by abrasion, and a thin In/Ga film or Al foil was applied to ensure good contact with the electrode. The sample was placed in a Teflon cell, and a hydride layer was formed by subsequent addition of 48% (w/w) aqueous HF (5 min). Subsequently, the HF solution was replaced by the electrolyte, which was a 1:1 (v/v) solution of 48% aqueous HF and ethanol and etched galvanostatically. Current densities of either 12.7 or 38.1 mA cm^{-2} were applied for 6.5 min. These etching conditions were chosen to produce highly uniform PS layers, which are stable under the reaction conditions used for the hydrosilylation, and to minimize cracking of the porous layer, rather than to optimize the luminescence properties. The porous silicon was then rinsed in deionized water (Millipore, 18 MΩ cm), immersed in 48% aqueous HF, rinsed in deionized water, dried in a stream of dry nitrogen, immersed in hexane for a few min, dried again in a stream of nitrogen, and finally stored under vacuum. Any residual water in the pores was removed by heating to ca. 100 °C for at least 3 h on a standard vacuum line using only grease-free joints, e.g., Young's taps.

To produce deuterium-terminated porous silicon (PS−D), a clean one-side abraded Si(100) sample was placed in a Teflon cell and a deuterium layer was formed by a subsequent addition of 40% DF in D_2O. After a few minutes, an equivalent amount of C_2H_5OD was added, and subsequently, a current density of either 12.7 or 38.1 mA cm^{-2} was applied. After 6.5 min, the sample was rinsed with D_2O, dried in a stream of nitrogen, and finally heated to ca. 100 °C for at least 3 h on a grease-free vacuum line to remove trace water. Generally we employed a current density of 12.7 mA cm^{-2} to produce hydrogen-terminated porous silicon (PS−H) and 38.1 mA cm^{-2} for deuterium-terminated material (PS−D) for experiments in which we were interested in studying the effect of hydrosilylation on the infrared spectra. This is because, as discussed below, these current densities produce similar intensities of the Si−H_x and Si−D_x stretching features in the FTIR spectra. A larger current density is required to produce the same intensity of the PS−D band because the oscillator strength of the Si−D vibration is lower (vide infra). A few experiments (Figure 1), in which we were studying the spectroscopy of PS−H and PS−D rather than the effect of hydrosilylation, were carried out with 12.7 mA cm^{-2}/(6.5 min) for PS−D for comparison of the H/D site densities. We also prepared some PS−H samples using HF(aq) diluted to 40% for comparison with the DF, which was only available at 40% (w/w).

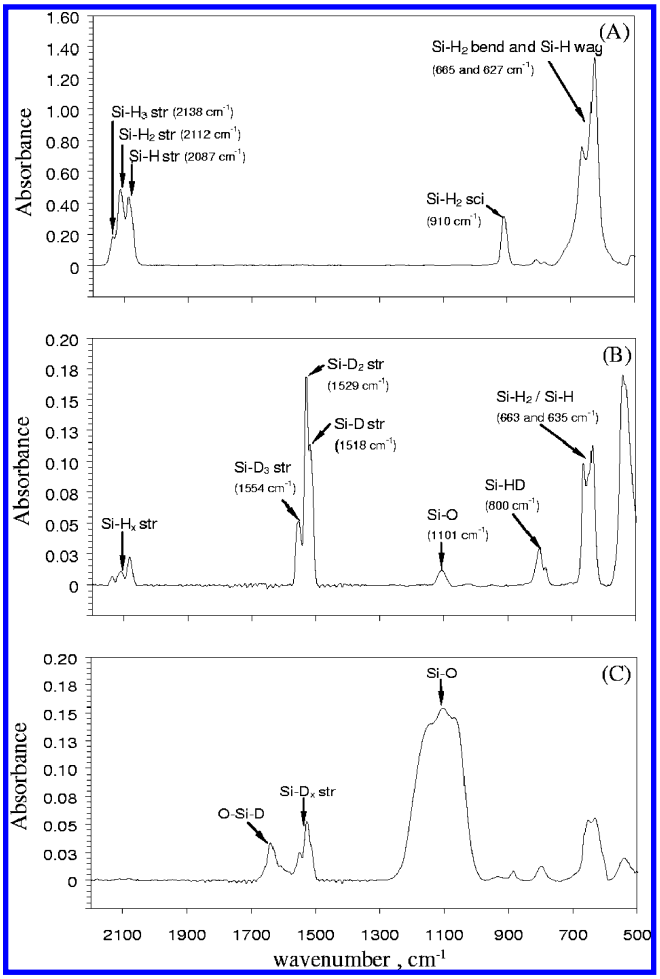

Figure 1. Baseline-corrected FTIR spectra of hydrogen- and deuterium-terminated porous silicon. Freshly prepared PS−H (A) and PS−D (B) samples and (C) an oxidized PS−D surface. In all spectra the background was a piece of unetched single-crystal wafer. The resolution is 4 cm^{-1}, and 32 scans have been co-added and averaged.

An IR spectrum of each porous silicon sample was recorded before further use. If contamination was present as indicated by low-intensity C−H vibration modes in the 2900−3000 cm^{-1} region, it was easily removed by rinsing the sample in hexane

and/or CH_2Cl_2. If the IR spectrum indicated substantial amounts of oxidation, the sample was reetched by immersing it in a 1:1 (v/v) solution of 48% aqueous HF and EtOH (or 40% DF in D_2O and EtOD) for a few minutes.

Formation of Monolayers. To avoid possible contamination of the samples by adventitious hydrocarbons, all reactions were performed under strict Schlenk line conditions, using entirely grease-free joints (Young's taps), and the vacuum line was isolated from the rotary pump by a liquid nitrogen-cooled trap. A wide variety of solvents have been used for the formation of 1-alkene monolayers on H-terminated Si(100) surfaces[8] and porous silicon.[26] Sieval et al. showed that well-ordered monolayers on H-terminated single-crystal Si(100) can be formed in toluene, xylene, cumene, *tert*-butylbenzene, and mesitylene.[8] The latter was identified as the solvent of choice, since the quality of the monolayer was high at significantly lower 1-alkene concentrations (down to 2.5% (v/v)). Since toluene, which is cheaper than mesitylene and available at high isotopic purity, was found to give high-quality monolayers from 10% (v/v) solutions,[8] we chose toluene as the solvent for most of the hydrosilylation reactions.

To perform a thermally induced reaction, a porous silicon sample was added to a 10% (v/v) solution of alkene and organic solvent (toluene or benzene), and subsequently the solution was heated at reflux for ~18 h. After the reaction, samples were rinsed with toluene followed by dichloromethane (2×) and dried in a stream of nitrogen. In the case of benzene, samples were rinsed with dichloromethane (2×) only. Some reactions were also carried out using neat 1-alkenes; these reactions were carried out at the same temperature as the toluene reflux (ca. 110 °C). Previous workers have obtained monolayers at porous silicon by thermal hydrosilation using, e.g., neat reagent and slightly lower temperatures that show very little oxidation.[25]

To investigate the role of trace oxygen and light in the initiation step some reactions were carried out in the dark and with freeze−pump−thaw degassed solutions. Traces of oxygen and possible peroxides in the undec-1-ene/toluene reaction mixture were removed in a two-step process: the reaction mixture was poured over a neutral alumina column (BDH, Poole, U.K.; neutral Brockmann grade I) and collected in a Schlenk flask. This Schlenk flask was subjected to three freeze−pump−thaw cycles (using a liquid N_2 Dewar flask) on a grease-free vacuum line. Finally, the porous Si chip was inserted under a flow of N_2, and the hydrosilylation reaction was performed under reflux as above.

Lewis acid catalyzed hydrosilylation reactions were performed in a horizontally oriented Schlenk flask. A few drops of $EtAlCl_2$ (1.0 M in hexanes), and subsequently a few drops of the neat alkene concerned, were carefully added onto a freshly prepared porous silicon sample using a syringe inserted into the flask. After 18 h, the excess of unreacted alkene and $EtAlCl_2$ was removed by rinsing with ethanol, deionized water and dichloromethane (2x).

Infrared Spectroscopy. Spectra (unpolarized) were obtained using an ATI Mattson Genesis Series FTIR spectrometer fitted with a deuterated triglycine sulfate (DTGS) detector in the normal transmission alignment. Spectra of both alkylated and unmodified porous silicon were referenced against an unetched piece of Si(100) wafer and have been baseline-corrected. The resolution is 4 cm^{-1} and 32 scans have been co-added and averaged. The integrated peak intensity, denoted as *A*, was calculated by using the integration option of the instrument-supplied software, WinFIRST.[64] A few spectra were recorded at higher resolution (0.25 cm^{-1}, Figure 2) using a Bio-Rad Excalibur spectrometer with an MCT detector and also baselined with the instrument-supplied (Merlin) software.

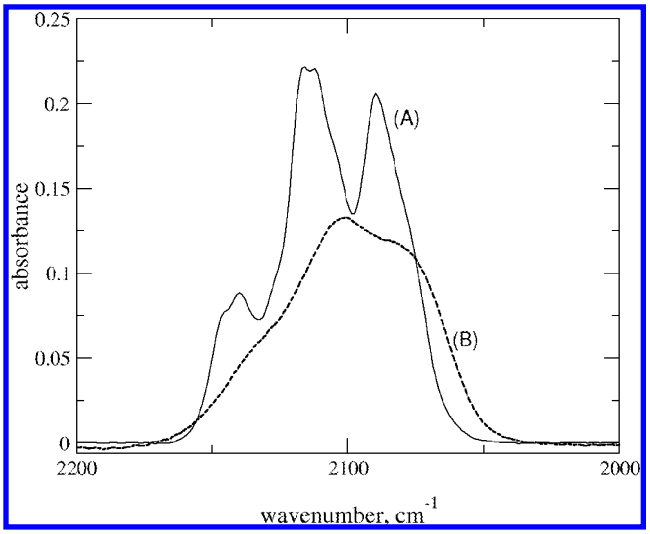

Figure 2. High-resolution (0.25 cm^{-1}) FTIR spectra of the $Si-H_x$ stretching bands on PS−H before (A) and after (B) thermal alkylation with 10% (v/v) undec-1-ene in toluene. In both spectra the background was a piece of unetched single-crystal wafer. The resolution is 0.25 cm^{-1}, and 40 scans have been co-added and averaged.

To compare different samples, the integrated absorbances were normalized with respect to the integrated absorbance of the $Si-H_x$ vibrations at 2100 cm^{-1} before the alkylation reaction ($A(Si-H_x)_0$), and are denoted as A_n. This enables us to compare integrated absorbances between samples since $A(Si-H_x)_0$ is proportional to the number of sites available for reaction. In the case of the C−H vibrations at 2925 cm^{-1}, the normalized integrated peak intensity $A_n(C-H)$,

$$A_n(C-H) = \frac{A(C-H)}{A(Si-H_x)_0} \quad (1)$$

yields the degree of alkylation (Equation 1). The subscript 0 in this equation and throughout the text indicates a quantity relating to the sample before reaction with alkene.

NMR Spectroscopy. Deuterated solvents were assessed for isotopic purity by ^1H NMR using a 500 MHz spectrometer (JEOL, Lambda 500). Benzene-d_6 and toluene-d_8 contained traces of C_6D_5H and $C_6D_5CD_2H$.

Computational Methods

Assignment of the IR spectra was aided by density functional and ab initio calculations on small molecule models of silicon surface. It has previously been observed that small silicon clusters provide reasonable models of the localized vibrational modes.[65−67] Calculations were performed without symmetry assumptions using either the Titan program package[68] or GAMESS/ PC-GAMESS.[69,70] Geometries and harmonic frequencies were evaluated using DFT calculations at the B3LYP/6-31G(d) or HF/6-31G(d) levels. The default grids of both DFT programs were used and no significant differences in optimized geometries were found. Titan does not allow one to obtain the intensities of vibrational modes at DFT level when the problem is solved by the (default) analytic method of frequency calculation. As a result, the calculations were performed using a numerical method by applying the option 'NMDER=2'.

To mimic the solid surface while minimizing the computational cost, the hydrogen atoms on the model cluster that do not correspond to those on the actual surface ('X') were replaced by tritium atoms or pseudo-hydrogen atoms of mass equivalent to Si (denoted as Q, available only in GAMESS). Depending on which aspect of the system was of interest, different model Si clusters were used. Small clusters of the form $SiX_3SiH_2SiX_3$ and $SiX_3SiD_2SiX_3$[62] were adequate to compute the ratio of integrated absorbances of Si−H/D stretches on porous silicon. In these calculations, the pseudo-hydrogen atom mass was set equal to that of silicon to avoid intensity effects from an unphysical coupling of the Si-D and Si-T modes. To compute the normalized intensity of the C−D stretch in an undecyl chain with a deuterium atom at the β-carbon on a silicon surface, the Si atom of the C−Si bond was connected to just three SiX_3 groups. This model is referred to as $Si_4X_9C_{11}H_{22}D$. In cases where information regarding the modes of both the surface and alkyl chain was required, i.e., to probe the interactions between Si−H and C−H stretching modes, another model was used; the length of the alkyl tail was reduced from 11 to 4 atoms for reasons of computational cost, while the silicon-cluster was enlarged to 13 atoms. The surface was ⟨111⟩ orientated, for simplicity and computational considerations, resulting in 7 surface Si−H bonds and 15 tritium atoms ($Si_{13}T_{15}H_7$). The alkyl tail, if present, was attached to the central silicon atom, leaving 6 unreacted surface Si−H sites. In this case, X = T is sufficient because Si−H and Si-T modes do not couple strongly.[66,67]

Results and Discussion

To test the radical chain mechanism for the formation of Si−C bonded monolayers on hydrogen-terminated porous silicon FTIR spectroscopy was used to detect incorporation of deuterium originating from the surface termination into the monolayer. First, we discuss the preparation of the deuterated surfaces and then investigate the possibility of H/D exchange between the surface and the solvent, in the absence of alkene, but under the conditions of the reaction (refluxing toluene or benzene). Next, we investigate whether deuterium can be transferred from the solvent to the monolayer during the alkylation reaction. Finally, we test directly whether the transfer of deuterium atoms from the surface to the monolayer occurs for both thermal and Lewis acid catalyzed reactions and compare the intensity of the C−D vibrational spectroscopic features with ab initio and density functional theory (DFT) calculations on small-molecule models of the porous silicon surface.

Comparison of Deuterium-Terminated (PS−D) and Hydrogen-Terminated (PS−H) Porous Silicon. The IR spectrum of hydrogen-terminated porous silicon (PS−H) shows bands at 2087, 2112, and 2138 cm^{-1}, which are attributed to Si−H, $Si-H_2$, and $Si-H_3$ stretching modes, respectively (Figure 1, spectrum A).[62,71] Other well-resolved features of the absorption spectrum include the $Si-H_2$ scissors mode (910 cm^{-1}) and $Si-H_2$ bending and Si−H wagging modes (665 and 627 cm^{-1}, respectively). The experimental integrated absorbance of the $Si-H_x$ stretching modes of a porous silicon sample prepared at 12.7 mA cm^{-2} for 6.5 min lies in the range 4−7 cm^{-1}. The IR spectrum of a deuterium-terminated porous silicon (PS−D) sample (Figure 1, spectrum B) shows two sets of three peaks, one at 1518, 1529, 1554 cm^{-1}, which corresponds to the Si−D, $Si-D_2$, and $Si-D_3$ stretching modes,[66,67] and another, less intense set around 2100 cm^{-1} is due to minority $Si-H_x$ species as described above. The low-intensity peak at ∼1100 cm^{-1} is due to small amounts of silicon oxide. Si−HD and Si−H wagging modes are resolved as well.[62] The use of DF in D_2O and EtOD and 38.1 mA cm^{-2} for 6.5 min in the porous silicon preparation resulted in integrated absorbances between 1−2 and 4−7 cm^{-1} for $Si-H_x$ and $Si-D_x$, respectively. For the majority of the experiments described below we employed a current density of 38.1 mA cm^{-2} to prepare PS−D in order to maximize the intensity of the Si−D features. The only exceptions were the experiments of Figure 1 in which we compared the density of D and H sites on PS using the same current density of 12.7 mA cm^{-2} for both PS−H and PS−D. The spectra of the PS−D surfaces produced in this study are similar to those published in a previous report[72,73] except in one aspect; these authors reported that the structures of the absorption bands of the Si−H and Si−D stretching modes are similar. However, we observed a difference in the intensity ratio of the different stretching modes for the PS−H and PS−D surfaces. In the case of PS−H surfaces, the order of peak intensities observed is $Si-H_2$ > Si−H > $Si-H_3$, while on our deuterated surfaces we find $Si-D_2$ > Si−D > $Si-D_3$ and Si−H > $Si-H_2$ > $Si-H_3$. Approximate values for the ratios of these intensities are required to calculate the total relative abundance of Si−H and Si−D species as described below. Given the low density of Si−H on the PS−D surface, it is likely that the relative abundance of Si−H can be explained as a statistical effect. Since $Si-H_3$ is still observed despite the H/D ratio being ca. 1:10 (see below), the distribution is not purely statistical and the origin of the relatively high intensity of $Si-H_3$ is not clear to us, but may be an isotope effect dependent on the details of the reaction of protons from HF with the surface during the etching process. Since the HF and DF solutions were provided at concentrations of 48 and 40%, respectively, by the manufacturer, we made a comparison of FTIR spectra of PS−H samples grown from 40 and 48% HF. These showed no difference in the shape of the $Si-H_x$ band and only a 6% drop in intensity on diluting the HF solution to the same concentration (40%) as the DF solution.

To calculate the ratio of H:D atoms using the measured intensities, the relation between the oscillator strength and the reduced mass of both systems is needed. Using various H-terminated Si clusters as models (more details of this calculation can be found in the section on computational models below), the ratio of the integrated absorbance of all the Si−H/Si−D stretches was found to be 1.89 at the B3LYP/6-31G(p)-level. This number was obtained using a ratio of 3:3:1 for the relative abundances of the SiH, SiH_2, and SiH_3 bands in the $Si-H_x$ stretching region based on the assignment of these bands in the experimental PS−H spectra by previous workers[66,67] and the observed intensity pattern. It is worth noting that this ratio is only weakly dependent on the relative abundances, and therefore the precise assignment of the individual $Si-H_x$ modes is not critical for the analysis in this report. Using this theoretical ratio of oscillator strengths, it was found that for a current density of 12.7 mA cm^{-2} (6.5 min) the use of deuterated media results in $N(D)/N(H) \approx 1.30$, where N is the number of atoms on the PS−H and PS−D surfaces prepared from 40% HF and 40% DF, respectively. The effect of increasing the HF concentration to 48% was ca. 6%. Matsumoto et al. reported a smaller excess of D sites; their observed ratio is $N(D)/N(H) = 1.06$,[71] under broadly similar etching conditions on 3−5 Ω cm resistivity p-Si. The reason is not clear, but presumably relates to an isotope effect on one or more steps in the etching process.

Approximately 92% of the Si−H/Si−D sites on PS−D were D-terminated, as determined from the integrated absorbances of the $Si-H_x$ vs $Si-D_x$ moieties. This observation can be rationalized on the basis that the isotopic purity of the DF/D_2O

was less than 100% and the anodization was performed in an open cell. Further, kinetic isotope effects leading to preferential reaction of surface sites with protons from HF are possible.

Finally, it is worth noting that the hydrogen atoms present in $Si-H_x$ moieties on a PS−D surface are chemically available as shown by oxidation of a PS−D sample by immersion for 5 h in D_2O/EtOD (Figure 1, spectrum C). The combination of ethanol/water is known to result in oxidation of porous silicon; the role of the ethanol is to wet the hydrophobic pores.[74] The high-intensity peak at ∼1100 cm^{-1} is attributed to oxide, while the peak at ∼1640 cm^{-1} corresponds to O−Si−D stretching modes. The region around 2100 cm^{-1}, corresponding to $Si-H_x$ stretching vibrations, is peak-free, although absorptions between 600 and 700 cm^{-1} suggest that the oxidized sample retains a small number of H-terminated sites.

Isotopic H/D Exchange Experiments in Toluene and Benzene. Because the solvent is a potential source for hydrogen atoms (Scheme 1), we investigated whether H or D atoms can be transferred between the solvent and the surface under typical hydrosilylation conditions, i.e., refluxing benzene or toluene in the absence of 1-alkenes. If this is the case, then this would have to be taken into account in using deuterium labeling to follow the fate of the surface H/D atoms during hydrosilylation of an alkene.

PS−H samples were refluxed for 18 h in either benzene-d_6 or toluene-d_8. No $Si-D_x$ stretching vibrations (expected between ∼1530 and ∼1560 cm^{-1})[71] were found in the FTIR spectrum of a PS−H sample after the reflux (data not shown), indicating that no D atoms from the solvent are abstracted by surface-bound silyl radicals. PS−D samples were also refluxed in nondeuterated solvents to determine whether D atoms from the silicon surface can be incorporated into the solvent molecules. For both toluene and benzene, the integrated absorbances of the $Si-H_x$ and $Si-D_x$ stretching vibrations were unchanged after reflux. In addition, the total number of sites, either hydrogen- or deuterium-terminated, was unaffected by the process of refluxing. This is consistent with the mechanism in Scheme 1 in the sense that if it were necessary to have a separate initiation event for each alkyl species which bonds to the surface, one might expect that under reflux there would be detectable H/D exchange between the surface and solvent even in the absence of alkene.

Thermal Reaction of 1-Alkenes with PS−H in Toluene and Benzene. If the hydrosilylation of 1-alkenes on the silicon surface does involve the abstraction of hydrogen atoms from the solvent (Scheme 1, arrows 1, 2, and 4), it is likely that benzene, which lacks easily abstracted hydrogen atoms, would be a much poorer choice of solvent than toluene, which ranks among the best solvents for this reaction.[8] To test this idea, the monolayer formation reaction was performed both in benzene and toluene with dilute solutions of undec-1-ene. The characteristic absorptions in the 2900 cm^{-1} region due to C−H vibration modes (∼2958, ∼2925, and ∼2855 cm^{-1}) and those around 2100 cm^{-1} due to the $Si-H_x$ stretching vibrations were observed as previously reported.[4,24] The peak at 1100 cm^{-1} is attributed to Si−O, while the peak at ∼1470 cm^{-1} corresponds to the CH_2 scissors vibrations. The integrated intensities of the alkyl bands are collected in Table 1.

To compare degrees of alkylation, the integrated absorbances, normalized with respect to the integrated peak intensity of the $Si-H_x$ vibrations before the modification, were determined according to eq 1. Intensities of the $Si-H_x$ vibrations after reflux were also normalized in an analogous manner. In all cases there is a loss of $Si-H_x$ intensity upon reaction ($A_n(Si-H_x) \sim 0.8$), but a more precise quantification is difficult, due to some overlap of the $Si-H_x$ and O−Si−H bands.

TABLE 1: Thermal Alkylation of PS−H with Undec-1-ene. Normalized Integrated Absorbances, A_n(C-H), of the C−H Stretching Modes of Alkylated PS−H Samples Prepared by Heating 1-Alkenes in Different Solvents (O Indicates an Open System, i.e., Heated to Normal Boiling Point; S, a Sealed System)

solvent	system	A_n(C−H)
benzene	O, reflux at 79 °C	2.43 ± 0.10
benzene	S, ca. 110 °C	2.99 ± 0.45
benzene-d_6	S, ca. 110 °C	2.23 ± 0.52
toluene	O, reflux at 110 °C	2.44 ± 0.10
toluene-d_8	O, reflux at 110 °C	2.46 ± 0.52

The overall efficiency of monolayer formation in both benzene and toluene can be deduced from the total integrated absorbance of the C−H stretching modes of the methylene and methyl moieties of the undecenyl chain. This value, A_n(C−H), is presented in Table 1. Taking account of sample-to-sample variations that are intrinsic to the use of PS, the amount of covalently bound alkyl chains is independent of the solvent (benzene vs toluene), isotopic substitution in the solvent (nondeuterated vs perdeuterated solvents), and reaction pressure/temperature (open and sealed reaction vessels of benzene). In summary, variation of the reaction medium in a variety of ways, including the absence or presence of easily abstracted hydrogen atoms, does not affect the extent of monolayer formation by hydrosilylation on porous silicon to a significant degree.

Thermal Reaction of 1-Alkenes with PS−H in Deuterated Solvents. In this type of experiment we looked for C−D stretching vibrations in the IR spectra after hydrosilylation as an indication of a possible role of solvent molecules as a source of hydrogen atoms for the carbon radical (Scheme 1, arrow 2). The wavenumber of the symmetric stretching vibration in CD_4 is 2109 cm^{-1},[75] which is, unfortunately, in the region of the $Si-H_x$ stretching vibrations. However, a difference might be expected in the shape or the intensity of peaks in the 2100 cm^{-1} region in comparison with nondeuterated solvents. Since we have shown (vide supra) that hydrogen atoms are not transferred between the surface and the solvent, abstraction of hydrogen/deuterium atoms by the carbon radical (Scheme 1, arrow 2) from the solvent would show up as increased normalized intensity, A_n(2100).

The normalized intensities in the 2100 cm^{-1} region after hydrosilylation were $A_n(2100) = 0.77 \pm 0.12$ in deuterated solvents (toluene-d_8 and benzene-d_6 data combined) and 0.79 ± 0.07 in nondeuterated solvents. The intensity in this region was therefore identical, and any contribution of C−D stretching modes must be less than the uncertainty. The observed scatter was largely associated with variations in the amount of oxidation occurring. No other differences in the FTIR spectra between deuterated and nondeuterated solvents were observed. In all cases the characteristic $Si-H_x$ triplet changes into a single broad peak at ∼2095 cm^{-1} upon alkylation (Figure 2). A small increase in intensity on the low wavenumber side of the peak, previously assigned to Si atoms bonded to both C and H, is also observed.[18,24]

Thermal Reaction of 1-Alkenes with PS−D. The abstraction of hydrogen atoms from the PS surface in the thermally induced alkylation can be studied using PS−D samples and analyzing the region around 2100 cm^{-1} in the IR spectrum for possible C−D stretching modes. This can be done in a quantitative way as the intensity of the potentially troublesome $Si-H_x$ bands on the PS−D surfaces prepared in this report is relatively small.

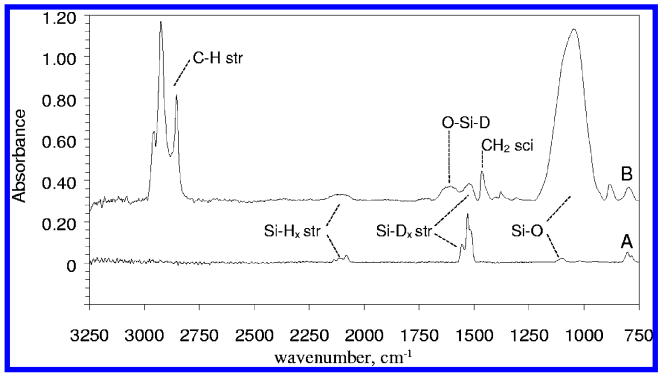

Figure 3. Baseline-corrected FTIR spectra of a PS−D sample before (bottom, A) and after (top, B) hydrosilylation in 10% (v/v) undec-1-ene in toluene. The top spectrum is offset by 0.3 absorbance units. In both spectra the background was a piece of unetched single-crystal wafer. The resolution is 4 cm^{-1}, and 32 scans have been co-added and averaged.

TABLE 2: Thermal Alkylation of PS−D with Undec-1-ene, Incorporation of D Atoms into C−D Bonds from the PS−D Surface As Measured by the Normalized Integrated Absorption, A_n(2100), and the Degree of Alkylation, A_n(C−H)[a]

solvent	A_n(2100)	A_n(C−H)
toluene	1.54 ± 0.21	2.96 ± 0.20
benzene	1.67 ± 0.39	3.37 ± 0.42
neat	1.53 ± 0.25	3.36 ± 1.17

[a] A_n(2100) denotes the features around 2100 cm^{-1} which, in principle, may be due to both Si−H_x and C−D stretching modes. A_n values were computed using eq 2 to account for the difference in intensities of Si−H and Si−D modes.

A typical spectrum of an undec-1-ene-derived monolayer on PS−D is given in Figure 3.

Upon reaction, C−H stretching vibrations around 2900 cm^{-1} and CH_2 scissor vibrations at ∼1470 cm^{-1} appear, in addition to oxide-related features at ∼1100 and 1580−1690 cm^{-1}. A normalized integrated absorbance (A_n)

$$A_n(\mathrm{C{-}H}) = \frac{A(\mathrm{C{-}H})}{A(\mathrm{Si{-}H}_x)_0 + gA(\mathrm{Si{-}D}_x)_0} \qquad (2)$$

which measures the degree of alkylation, can be calculated from the C−H stretching features after alkylation (A(C−H)) and the absorption bands from the hydrogen-terminated surface before alkylation (A(Si−H_x)$_0$, A(Si−D_x)$_0$). The subscript 0 indicates a quantity relating to the sample before reaction.

The numerical factor $g = 1.89$ takes account of the isotope effect on the integrated absorbance and is obtained from computations on small-molecule models below (see Table 5). The data for the degree of alkylation according to eq 2 is presented in Table 2. In addition, the integrated peak intensity in the 2100 cm^{-1} region after modification, A_n(2100) relative to this total number of sites, is presented, which enables quantification of the number of C−D bonds formed by the radical chain mechanism (Scheme 1).

For both solvents, an increase in intensity around 2100 cm^{-1} is observed upon alkylation, which is denoted by A_n(2100) > 1.00. Hydrosilylation was also performed in neat undec-1-ene as well, and the data show that the degree of alkylation is comparable with the experiments in 10% (v/v) alkene solutions. These data imply that, apart from the Si−H_x modes observed at ∼2083, ∼2112, and ∼2138 cm^{-1}, additional C−D bonds are being formed and observed (and part of the SiH_x lost), which can only be the case if deuterium atoms are abstracted from the PS−D surface and incorporated into the alkyl chain.

The broadness of the peak around 2100 cm^{-1} may be explained by the possibility that reaction with the surface can lead to heterogeneous broadening of Si−H_x and C−D modes. Boukherroub and co-workers suggested this possibility in order to rationalize the apparent disappearance of the Si(111)−H stretch without the appearance of new absorptions upon reaction with aldehydes.[76] Such broadening is also observed in other modifications, e.g., in the electrochemical modification of Si(111)−H by aryldiazonium ion.[11] In addition, simple physisorption of a hydrocarbon on the Si(111)−H surface results in an increase in the peak width of the Si−H monohydride stretch.[76]

Given the fact that a porous silicon surface contains mono-, di-, and trihydride groups, it is not surprising that the Si−H peaks are broad. In the case of alkylated PS, there is the additional possibility that the C−D bond interacts with Si−H_x bonds on the surfaces, resulting not only in peak broadening and overlap but also in a transfer of intensity. Figure 2 shows the Si−H_x stretching band of PS−H at higher resolution before and after alkylation by 10% (v/v) undec-1-ene in toluene. Aside from the reduction in the total integrated intensity, two effects of alkylation are apparent: the three peaks merge into a single broad band, and there is a net increase in intensity on the low-wavenumber side of the band, which has previously been assigned to the influence of Si−C bonds on the Si−H frequency.[24,62] The influence of oxidation also has to be taken into consideration as it can be seen in Figure 3 that the largest increase in the 2100 cm^{-1} region upon alkylation of PS−D is found for the higher wavenumbers, adjacent to the region in which O−Si−H modes can be expected. As a result, part of the intensity might be the result of the presence of an O−Si−H mode. However, this cannot explain an increase in Si−H intensity overall since oxidation is known to result in a net loss of Si−H intensity. Additionally, the oscillator strength of the O−Si−H modes is not much higher than that of the Si−H_x modes.[3,26,62,74]

In an attempt to remove trace Si−H_x, which is one of the possible two contributions to the bands in the 2100 cm^{-1} region, alkylated PS samples were lightly oxidized by immersing the sample into a 25% (v/v) EtOD in D_2O solution.[74] These conditions did not result in a significant change in shape and intensity of the broad peak at ∼2100 cm^{-1}, which is at least consistent with an assignment of the 2100 cm^{-1} feature to C−D species. However, since the alkyl monolayer will protect the sample against oxidation somewhat,[3,26] it is not safe to conclude from this observation alone that there is no Si−H_x attribution to the 2100 cm^{-1} peak. Attempts to preoxidize samples of PS−D to remove the trace Si−H were not useful due to the reduced amount of Si−D remaining for hydrosilylation and the possible contamination of the PS with the water/ethanol mixture, leading to extensive oxidation. We did observe, however, that the addition of 5% (v/v) D_2O to the toluene/undec-1-ene mixture used for thermal hydrosilylation did not affect the degree of alkylation significantly.

Thermal Reaction of Styrene with PS−D. It has previously been reported in a molecularly resolved STM study[56] that styrene favors the chain mechanism compared to a straight chain alkene, i.e., propene in the original work. This was rationalized on the basis of the stability of the carbon radical intermediate on the surface.

Thermal hydrosilylation of styrene was performed as for undec-1-ene. However, styrene is very susceptible to polym-

TABLE 3: Thermal Alkylation of PS−D with Styrene. Integrated Absorbances (A, cm^{-1}) of Several Modes before and after the Thermal Reaction of Styrene with PS−D and the Degree of Alkylation, A_n(C−H)[a]

concentration and solvent	A(Si−H$_x$)	A(2100)	A(C−H)	A_n(2100)	A_n(C−H)
neat styrene	1.58 ± 0.02	1.45 ± 0.71	10.4 ± 4.8	0.93 ± 0.47	0.89 ± 0.42
10% in toluene	1.93 ± 0.35	4.16 ± 0.55	5.44 ± 1.6	1.93 ± 0.16	0.40 ± 0.13
10% in benzene	1.78 ± 0.14	2.96 ± 0.32	6.76 ± 3.5	1.66 ± 0.12	0.44 ± 0.23

[a] A_n(2100) refers to the features around 2100 cm^{-1} which, in principle may be due to both Si−H$_x$ and C−D stretching modes. A_n values were computed using eq 2 to account for the difference in intensities of Si−H and Si−D modes.

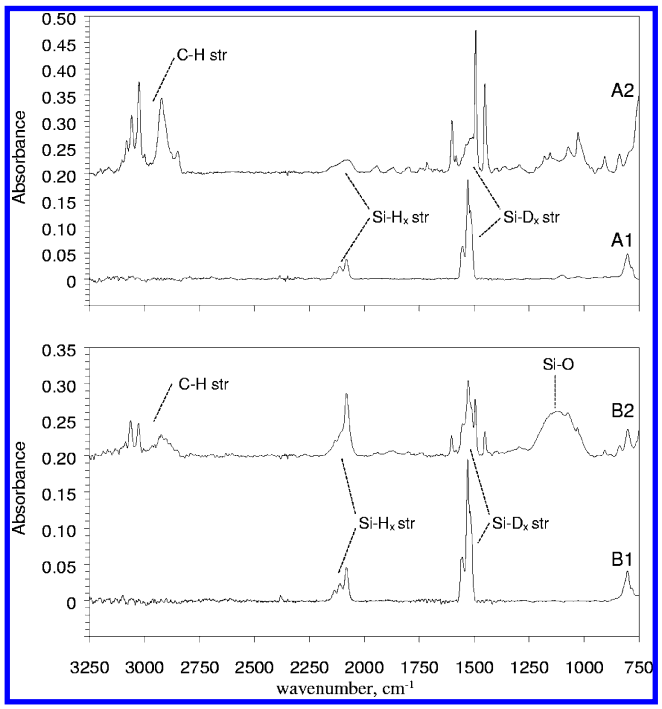

Figure 4. Baseline-corrected FTIR spectra of a styrene monolayer on a PS−D surface and corresponding PS−D surfaces before reaction (A1 and B1) and after reaction using neat (A2) and 10% (v/v) styrene in toluene (B2). In each panel the top spectrum is offset by 0.2 absorbance units for clarity. In all spectra the background was a piece of unetched single-crystal wafer. The resolution is 4 cm^{-1}, and 32 scans have been co-added and averaged.

erization, and even in the dilute (10% (v/v)) styrene solutions used, some polymerization took place. After 18 h reaction time, the viscosity of the solution was increased; however, the polymerized material was soluble and easily removed by washing. For both toluene and benzene the integrated peak intensity at 2100 cm^{-1} increases upon reaction (A_n(2100) > 1; see Table 3), although this increase seems slightly higher in the experiments with toluene. In this respect, the results of styrene and undec-1-ene are comparable; the integrated peak intensity in the 2100 cm^{-1} region increases upon reaction in both cases, which is an indication for the formation of C−D bonds.

There is a noticeable difference between styrene and undec-1-ene with regard to the peak shape of the absorptions at 2100 cm^{-1}. For undec-1-ene and other 1-alkenes, the peaks due to residual Si−H$_x$ broaden, sometimes to the extent that they cannot be resolved, and a single band is observed. For styrene, the peak did not broaden as dramatically; after the reaction, three peaks could still be distinguished at ∼2082, ∼2103, and ∼2134 cm^{-1} at approximately the same wavenumbers as before the reaction (spectrum B2 in Figure 4). Although it appears that the vibrational energies do not change upon the addition of styrene, the peaks are not as well resolved, which may be due to small amounts of C−D absorptions. The difference in the shape of the 2100 cm^{-1} region absorption peak between styrene and undec-1-ene can be rationalized on the basis that the degree of reaction is smaller; cf., A_n(C−H) data in Tables 2 and 3. The smaller degree of reaction with styrene is likely to result from its tendency to polymerize under the reaction conditions employed here.

Source of the Radicals in the Thermal Hydrosilylation of PS−H and PS−D. So far we have discussed the fate of H/D atoms and the propagation of the chain, but not the source of the radicals, i.e., the initiation step. There are several possibilities: (1) photochemical initiation, (2) reaction of trace oxygen with the H-termination, and (3) thermal processes involving the breaking of Si−Si or Si−H bonds by reactions of holes or electrons. Certainly, photochemical initiation has been reported for the derivatization of single crystal[9,22,23] and porous silicon by 1-alkenes.[19] However, the source of the radicals in the thermal hydrosilylation reaction employed in this and other reports[8,24] is not clear. To test the various possibilities, we have determined the extent of alkylation of porous silicon by 10% (v/v) undec-1-ene in toluene under conditions where stray light, water and/or oxygen, and peroxides were carefully excluded by freeze−pump−thaw degassing of the reaction mixture after passing down a column of neutral alumina. We find essentially no difference in the extent of alkylation with careful exclusion of trace water or stray light by enclosing the Schlenk flask in black paper. However, when the reaction is carried out with rigorous degassing by the freeze−pump−thaw method on the vacuum line and the 1-alkene/toluene is passed through neutral alumina to remove peroxides,[77,78] we find that the extent of alkylation drops from 2.51 ± 0.25 (Table 1) to 0.41 ± 0.10 in the absence of oxygen. Further, about 90% of the intensity of the Si−H stretch remains and the peaks are well-resolved and not broadened as observed at higher levels of alkylation. We therefore conclude that the major initiation step in the thermal hydrosilylation reaction is a process involving abstraction of hydrogen atoms from the surface by trace oxygen. The promotion of molecular hydrosilylation reactions by oxygen is known,[79] and it appears reasonable to conclude that a similar process occurs on the hydrogen-terminated silicon surface.

Lewis Acid Catalyzed Reaction of Undec-1-ene with PS−D. Buriak and co-workers have reported a mild and quite general approach for covalent modification of the surface of porous silicon through $EtAlCl_2$-catalyzed hydrosilylation of readily available 1-alkynes and 1-alkenes.[26,77,78,80] Asao et al. proposed a mechanism for the molecular version of this type of reaction, in which the H atom shifts from the Si to the C atom of a Lewis acid−alkene intermediate.[63] This should also lead to incorporation of D atoms at the β-carbon on PS−D surfaces. In comparison with the thermal alkylation in toluene, the degree of oxidation is very low in the case of the reaction with the Lewis acid ($EtAlCl_2$). In this reaction we can therefore expect a negligible contribution of O−Si−H modes to the broad peak at 2100 cm^{-1}.

Figure 5 depicts an FTIR spectrum of an undec-1-ene monolayer on a PS−D surface prepared with $EtAlCl_2$ as catalyst. Only a small absorption around 1100 cm^{-1}, specific for oxide

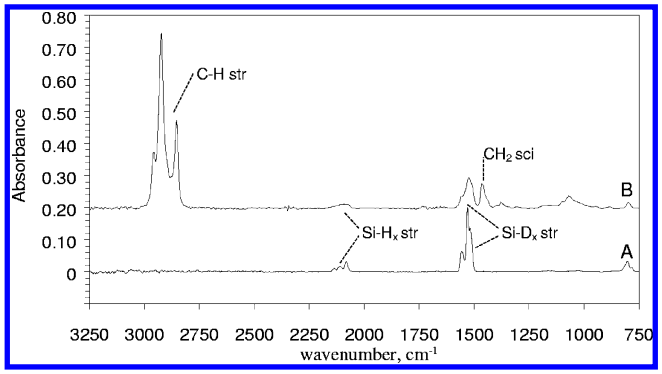

Figure 5. Baseline-corrected FTIR spectrum of an undec-1-ene monolayer on a PS−D surface prepared with Lewis acid (B) and the spectrum before reaction (A). The top spectrum is offset by 0.2 absorbance units. In both spectra the background was a piece of unetched single-crystal wafer. The resolution is 4 cm^{-1}, and 32 scans have been co-added and averaged.

formation, is observed, indicating that the use of Lewis acid indeed results in a very low degree of oxidation. There are several factors which favor this: (1) the reaction is carried out at ambient temperature, (2) no solvent is required which reduces the likelihood of introducing trace water and oxygen, and (3) the $EtAlCl_2$ reacts rapidly with trace water to form insoluble aluminum species.

Table 4 shows the relevant data of the Lewis acid catalyzed addition of undec-1-ene. The mean degree of alkylation of the three fresh samples is 2.00 ± 0.46. This is slightly lower than the average values for the thermal reaction of PS−D samples (see Table 2) in toluene (2.96 ± 0.20) and benzene (3.37 ± 0.42). The observation of a lower coverage in case of the use of Lewis acids is in line with the results of Boukherroub et al.[80]

The trends in the changes around 2100 cm^{-1} for the thermally induced and Lewis acid catalyzed addition of undec-1-ene are the same: in both methods an increased integrated peak intensity in the 2100 cm^{-1} region is observed upon hydrosilylation. Although there is some scatter between samples in the values of $A(Si-H_x)_0$ and $A(2100)$, in each case $A(2100) > A(Si-H_x)_0$. The main differences are a lower degree of alkylation in the Lewis acid catalyzed reaction but also a much lower extent of oxidation. These observations are again consistent with an assignment of the 2100 cm^{-1} feature to C−D stretching modes and support the proposed reaction mechanisms.[1,57]

Ab Initio and DFT Calculations. Since the vibrational frequencies of the $Si-H_x$, O−Si−H, and C−D bands are quite close, any of these modes might contribute to the observed broad feature at 2100 cm^{-1}. In addition, using the ratio of the integrated absorbances of Si−D and Si−H stretches to determine the composition of the surface with respect to D and H atoms requires knowledge of the ratio of the corresponding oscillator strengths (g in eq 2). Computed vibrational frequencies and intensities of models of deuterated surfaces as well as the interaction between the alkyl chains of a monolayer and the remaining $Si-H_x$ bonds were therefore helpful in interpreting the experimental results above. All the computed harmonic vibrational frequencies were scaled with the factors determined by Scott and Radom.[81]

(1) Ratio between A_n(Si−H) and A_n(Si-D). Due to the mass difference, the integrated absorbance of an Si−H stretching mode differs from that of an Si−D mode. In general, the absorbance integrated over a frequency interval should be inversely proportional to the reduced mass, μ, since the factor of $\mu^{-1/2}$ appears twice in the expression for the integrated absorbance: once in the frequency and once via the transition dipole. A calculation of the reduced mass requires a determination of the normal modes. Since the small models $X_3Si-SiH_3$, $(X_3Si)_2-SiH_2-SiX_3$, and $(X_3Si)_3-SiH$ have previously been found to be adequate for computing isotope effects on the frequency,[62] the calculations were performed on these molecules at the B3LYP/6-31G(d) level. The results are collected in Table 5. The X atoms are hydrogens whose only purpose is to satisfy the valence of Si atoms in the cluster, but are not otherwise of interest and are assigned a mass equal to that of silicon (Q) to avoid coupling with the $Si-H_x$ or $Si-D_x$ modes of interest.[62,65−67] It is worth noting that although use of X = tritium (T) is sufficient for many purposes,[66,67] it results in some coupling with Si−D modes and therefore cannot be used in calculations aiming to determine the relative integrated intensity of $Si-H_x$ and $Si-D_x$ modes. Table 5 contains the ratios of vibrational wavenumbers and intensities for $X_3Si-SiH_3$, $(X_3Si)_2-SiH_2-SiX_3$, and $(X_3Si)_3-SiH$. The ratio of intensities is close to 2. This is expected on general grounds since the reduced mass of the Si−H stretching modes should be dominated by the mass of the H atom. The value of $g = 1.89$ that was employed in eq 2 throughout the text was obtained by averaging over the results for SiH_3, SiH_2, and Si−H with weighting 1:3:3 reflecting the experimental spectra. However, the value was not very sensitive to this ratio (±0.02).

(2) Ratio between A_n(C−H) and A_n(C−D) and Estimation of A(2100). To get more insight into the origin of the broad peak in the 2100 cm^{-1} region, the ratio of the intensities of the C−H and C−D stretching vibration was calculated. Together with the experimental integrated absorbance of the C−H vibration, this theoretical ratio can be used to estimate the contribution of the C−D stretching vibration to the total integrated absorbance in the 2100 cm^{-1} region. Table 6 gives some details and relevant output data of calculations on the $Si(SiX_3)_3C_{11}H_{22}D$ model at two different levels. The calculated vibrational energy of the C−D bond at the B3LYP/6-31G(d) level is 2153.23 cm^{-1}, close to the ν(Si−H) region calculated at the same level (Table 5). Figure 6A shows the optimized structure of this model at the B3LYP/6-31G(d) level.

Using the HF/6-31G(d) model, the scaled vibrational wavenumber of the C−D band is quite close to the literature value of this mode in CD_4 (2109 cm^{-1}).[75] The ratio of the intensities of the C−H and C−D bands computed by DFT and HF methods differs by about 10%. The effect of replacing the T atoms by Si atoms is smaller than this uncertainty, as can be seen from the data in the last two rows of Table 6. This justifies the use of T atoms in some cases where the particular software package does not allow assignment of an arbitrary mass.

Table 7 compares the observed and calculated values of integrated absorbance in the 2100 cm^{-1} region after thermal hydrosilylation of undec-1-ene on PS−D. The values in the last column of this table were calculated as the sum of contributions from A(C−D) and $A(Si-H_x)$, rewritten in terms of experimentally accessible quanities, as

$$A(2100) = A(C-H)f + 0.8A(Si-H_x)_0 \qquad (3)$$

Equation 3 uses a value for $A_n(Si-H_x)$, taken from several experiments on alkylation of PS−H samples, of 0.8. The corresponding value on PS−D samples is not known but is expected to be similar. For the calculation of A(2100) the experimental value for A(C−H) and the calculated ratio $f = A(C-D)/A(C-H) = 1/53.2$ are used. From Table 7 it can be seen that the major part of the change in intensity in the 2100 cm^{-1} region can be accounted for satisfactorily by the formation

TABLE 4: $EtAlCl_2$-Catalyzed Alkylation of PS−D with Undec-1-ene; Experimental Peak Intensities (A, cm^{-1}) of Several Modes after Preparation of PS−D and after $EtAlCl_2$-Catalyzed Reaction of Undec-1-ene and the Degree of Alkylation, A_n(C−H) According to Equation 2

	after preparation of PS−D		after $EtAlCl_2$-catalyzed reacn of undec-1-ene		
solvent	$A(Si-H_x)_0$	$A(Si-D_x)$	$A(2100)$	$A(C-H)$	$A_n(C-H)$
neat undec-1-ene	1.47 ± 0.25	6.87 ± 0.73	1.54 ± 0.42	26.2 ± 3.8	2.00 ± 0.46

TABLE 5: Ratio of Vibrational Wavenumbers and Intensities of the Si−H and Si−D Stretching Modes of Various Small-Molecule Models of Hydrogen-Terminated Silicon (and Their Deuterated Equivalents), Calculated at the B3LYP/6-31G(d) Level[a]

molecule[b]	ν(Si−H)/ν(Si−D)	A(Si−H)/A(Si−D)
$(Q_3Si)_3SiH$	1.391	1.950
$(Q_3Si)_2SiH_2$	1.384, 1.397	1.889, 1.840
$(Q_3Si)SiH_3$	1.384, 1.384, 1.405	1.788, 1.788, 1.747

[a] Q denotes a pseudo-hydrogen atom with atomic mass equivalent to Si. When these contributions are weighted 1:3:3 for $Si-H_3$, $Si-H_2$, and Si−H, a mean value of the ratio of integrated intensities for $g = A(Si-H)/A(Si-D) = 1.89$ is obtained (eq 2). [b] All calculations using GAMESS.[69,70]

TABLE 6: Specification of the Calculation Method, Scaled Vibrational Energies (ν, cm^{-1}) and Computed Intensities (A, km mol^{-1}) of the C−H and C−D Modes of the $Si(SiX_3)_3C_{11}H_{22}D$ Model

X	level	ν(C−H)	ν(C−D)	A(C−H)	A(C−D)	A(C−H)/A(C−D)
T	B3LYP[a]	2988.11−2892.14	2153.23	767.56	14.43	53.2
T	HF[a]	2911.27−2834.21	2101.60	852.99	14.89	57.3
Q	HF[b]	2911.27−2834.21	2101.59	852.44	14.80	57.6

[a] Calculations using Titan.[68] [b] Calculations using GAMESS.[69,70]

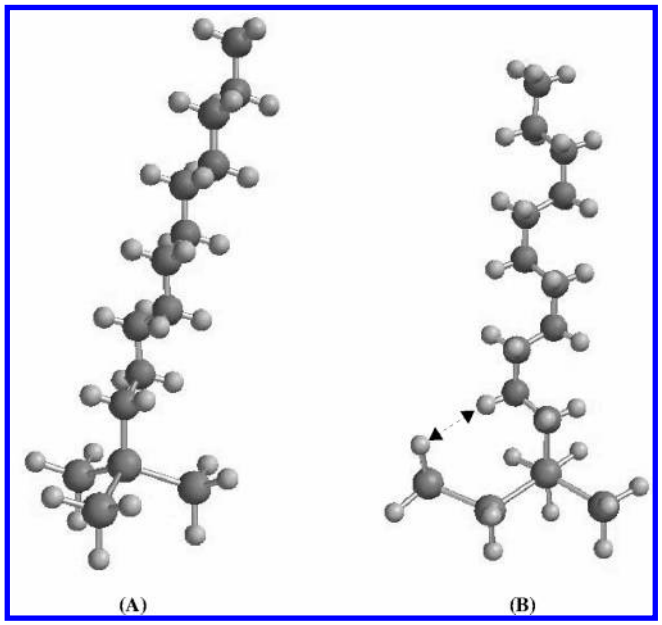

Figure 6. Optimized structures of (A) $Si_4X_9C_{11}H_{22}D$ and (B) $Si_5X_{10}HC_{11}H_{22}D$ at the B3-LYP/6-31G(d) level. (A) All denoted X are pseudo-hydrogen atoms terminating the silicon valences, but not representing atoms on the actual surface and are assigned masses equivalent to T. (B) The arrow indicates an interaction between the C−D and Si−H stretching vibrations discussed in the text. All other H atoms bonded to Si are pseudoatoms (X) which satisfy the valence of the Si atoms but are assigned higher masses in order to remove artifacts due to coupling with Si−H bonds of interest.

of a C−D bond via the radical chain mechanism of Chidsey and co-workers (illustrated in Scheme 1).[1] The difference may be the result of several factors; no account is made for the effect of small amounts of oxidation, and there is the possibility of an interaction between C−D and Si−H/D_x stretching vibrations leading to intensity changes. The latter possibility is neglected in the calculations based on the $Si(SiX_3)_3C_{11}H_{22}D$ model.

TABLE 7: Thermal Alkylation of PS−D with Undec-1-ene; Integrated Absorbances (cm^{-1}) in the 2100 cm^{-1} Region upon Thermal Reaction of Undec-1-ene with PS−D[a]

concn and solvent	expt A(C−H)	expt A(2100)	calcd A(2100)
neat undec-1-ene	41.8 ± 4.0	1.85 ± 0.06	1.77 ± 0.05
10% in toluene	42.0 ± 11.1	2.42 ± 0.19	2.05 ± 0.13
10% in benzene	42.4 ± 2.4	2.22 ± 0.13	1.90 ± 0.23

[a] The calculated value for the integrated absorbance at 2100 cm^{-1} is determined from eq 3 and the experimental integrated absorbance A(C−H).

(3) Interaction between C−D and Si−H. A possible explanation for the observed broadening of the peak in the 2100 cm^{-1} region upon alkylation is an interaction between the C−D and $Si-H_x$ stretching vibrations due to the close proximity of the hydrogens on the β-carbon to neighboring Si−H sites. Such an interaction may affect the frequency of the normal mode and also lead to intensity borrowing, which would affect the value of $A(2100)/A(Si-H_x)_0$. To study this possibility, a calculation (B3LYP/6-31G(d) level) was performed on the $Si(SiX_3)_3C_{11}H_{22}D$ model (Figure 6A) in which one X pseudoatom was replaced by an $SiHX_2$ group to make $Si_5X_{10}HC_{11}H_{22}D$ (Figure 6B). As expected, the C−D and $Si-H_x$ bonds give rise to two normal modes at 2151.1 and 2158.8 cm^{-1}, with intensities of 98.3 and 30.3 km mol^{-1}, respectively. These correspond to in-phase and antiphase stretching vibrations of the Si−H and C−D bonds indicated by an arrow in Figure 6B. For $Si(SiX_3)_3C_{11}H_{22}D$ (model A) where there is no possibility of such an interaction; the intensity of the C−D stretching vibration was only 14.43 km mol^{-1} (see Table 6). Calculations on the $Si_{13}X_{15}H_aD_b$ model indicate the contribution of a single Si−H bond, is between 74.3 and 67.9 km mol^{-1}. From these calculations it can be concluded that there is a significant interaction between the C−D and neighboring Si−H bond, resulting in increased intensities in the modes around 2100 cm^{-1} than in cases where these atoms do not have the possibility to interact.

To better represent the surface, calculations on a larger silicon cluster were performed (Figure 7). Parts A and B of Tables 8 give the wavenumber and integrated absorbances of the surface (Table 8A) and the alkyl chain (Table 8B) of calculations on the $Si_{13}X_{15}H_aD_bC_4H_cD_d$ model at the B3LYP/6-31G(d) level.

Figure 7B depicts the optimized structure of $Si_{13}X_{15}H_6C_4H_9$ at this level. The presence of a H-terminated surface shifts the vibrational energy of the C−D bond only 1−2 cm^{-1} as follows from comparison of the data in Tables 6 and 8b. Its intensity, however, is influenced to a larger extent by the presence of Si−H bonds. The calculation on the $Si(SiX_3)_3C_{11}H_{22}D$ model, an alkyl chain bonded on an Si−H free silicon cluster, gave an intensity of 14.43 km mol^{-1} for the vibrational intensity of the C−D bond, using the B3LYP functional and 6-31G(d) basis set. For the (shorter) alkyl tail on the Si_{13} cluster, the intensity of this mode is ca. 14% higher (16.49 km mol^{-1}; see Table 8b). It was observed that the C−D bond has strong interactions with the H atoms indicated by arrows in Figure 7B, which is

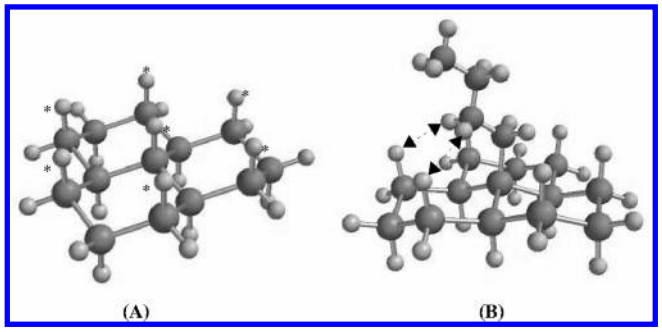

Figure 7. Optimized structures of (A) $Si_{13}X_{15}H_aD_b$ and (B) $Si_{13}X_{15}H_aD_bC_4H_cD_d$ at the B3LYP/6-31G(d) level. (A) The asterisks denote the hydrogen atoms (H_aD_b) of interest; the rest are pseudo-hydrogen atoms (X) which satisfy the valences of the Si cluster but are assigned masses equivalent to T to avoid artifacts due to coupling with Si−H modes of interest. (B) The arrow indicates an interaction between the C−D and Si−H stretching vibrations discussed in the text.

TABLE 8: Range of Scaled Vibrational Energies (cm^{-1}) and Summed Intensities (km mol^{-1}), Calculated at the B3LYP/6-31G(d) Level[a]

(A) Si−H and Si−D Stretching Modes of the $Si_{13}X_{15}H_aD_bC_4H_cD_d$ Model

a	*b*	*c*	*d*	*ν*(Si−H)	*ν*(Si−D)	*A*(Si−H)	*A*(Si−D)
6	0	9	0	2141.8−2120.9		493.2	
6	0	8	1	2138.4−2110.2		503.4	
0	6	8	1		1539.0−1526.4		281.0

(B) C−H and C−D Stretching Modes of the $Si_{13}X_{15}H_aD_bC_4H_cD_d$ Model

a	*b*	*c*	*d*	*ν*(C−H)	*ν*(C−D)	A(C−H)	*A*(C−D)
6	0	9	0	2992.0−2902.5		207.9	
6	0	8	1	2994.7−2901.3	2150.3	190.4	16.49
0	6	8	1	2991.9−2902.4	2152.1	191.1	8.78

[a] Calculations using Titan.[68]

the result of the staggered conformation seen looking down the C−Si bond with respect to the position of the H atoms on the β-carbons and the Si−Si bonds on the surface. Substitution of the 6 H atoms on the alkylated surface by D atoms gives an intensity of 8.78 km mol^{-1} for *A*(C−D). The latter result is expected, since the frequencies of the C−D and Si−D are well-separated.

To summarize, the calculations on model clusters indicate that there is a significant interaction between H/D atoms on the β-carbons and the surface termination. This interaction is most significant for C−D and Si−H stretching modes whose frequencies are very similar. This type of interaction can contribute to the broadness of the residual $Si-H_x$ stretching band observed on alkylated porous silicon.

Conclusions

Combined experimental data on the thermal hydrosilylation of deuterated porous silicon with 1-alkenes and theoretical investigations of alkylated silicon clusters support a radical chain mechanism[1,26,77,78] for the formation of covalent alkyl monolayers on porous silicon. In addition, the results of reactions carried out with strict control over the conditions (atmosphere, light, water) point to initiation of this reaction by trace amounts of oxygen. The Lewis acid catalyzed hydrosilylation reaction of porous silicon was also studied, and the expected incorporation of hydrogen atoms from the surface in the alkyl chain was observed. Finally, the frequently observed broadening of $Si-H_x$ vibrations left after the (partial) coverage of PS by hydrosilylation of alkenes is shown to have a contribution from the interaction between the $Si-H_x$ groups and the second CH_2 moiety in the monolayer.

Acknowledgment. We thank Dr. Dawei Guo (Wageningen University) for computational assistance. EPSRC for funding under Grants GR/M69104 and AF/990206 (B.R.H./A.H.) and The Research Council of Norway (L.H.L.). L.C.P.M.dS. thanks Wageningen University ("Stichting Wagenings Universiteits Fonds"), the Royal Institution of Engineers (Netherlands KIVI), and the Fundatie van de Vrijvrouwe van Renswoude for financial support.

References and Notes

(1) Linford, M. R.; Fenter, P.; Eisenberger, P. M.; Chidsey, C. E. D. *J. Am. Chem. Soc.* **1995**, *117*, 3145.
(2) Linford, M. R.; Chidsey, C. E. D. *J. Am. Chem. Soc.* **1993**, *115*, 12631.
(3) Buriak, J. M. *Chem. Commun.* **1999**, 1051.
(4) Buriak, J. M. *Chem. Rev.* **2002**, *102*, 1271.
(5) Sung, M. M.; Kluth, G. J.; Yauw, O. W.; Maboudian, R. *Langmuir* **1997**, *13*, 6164.
(6) Hovis, J. S.; Hamers, R. J. *J. Phys. Chem. B* **1998**, *101*, 9581.
(7) Boukherroub, R.; Wayner, D. D. M. *J. Am. Chem. Soc.* **1999**, *121*, 11513.
(8) Sieval, A. B.; Vleeming, V.; Zuilhof, H.; Sudhölter, E. J. R. *Langmuir* **1999**, *15*, 8288.
(9) Cicero, R. L.; Linford, M. R.; Chidsey, C. E. D. *Langmuir* **2000**, *16*, 5688.
(10) Effenberger, F.; Götz, G.; Bidlingmaier, B.; Wezstein, M. *Angew. Chem., Int. Ed.* **1998**, *37*, 2462.
(11) de Villeneuve, C. H.; Pinson, J.; Bernard, M. C.; Allongue, P. *J. Phys Chem. B* **1997**, *101*, 2415.
(12) Zazzera, L. A.; Evans, J. F.; Deruelle, M.; Tirrell, M.; Kessel, C. R.; McKeown, P. *J. Electrochem. Soc.* **1997**, *144*, 2184.
(13) Bansal, A.; Li, X.; Lauermann, I.; Lewis, N. S.; Weinberg, W. H. *J. Am. Chem. Soc.* **1996**, *118*, 7225.
(14) Ozanam, F.; Vieillard, C.; Warntjes, M.; Dubois, T.; Pauly, M.; Chazalviel, J.-N. *Can. J. Chem. Eng.* **1998**, *76*, 1020.
(15) Dubois, T.; Ozanam, F.; Chazalviel, J.-N. *Proc. Electrochem. Soc.* **1997**, *97-7*, 296.
(16) Gurtner, C.; Wun, A. W.; Sailor, M. J. *Angew. Chem., Int. Ed.* **1999**, *38*, 1966.
(17) Fidélis, A.; Ozanam, F.; Chazalviel, J.-N. *Surf. Sci.* **2000**, *444*, L7.
(18) Lie, L. H.; Patole, S. N.; Hart, E. R.; Houlton, A.; Horrocks, B. R. *J. Phys. Chem. B* **2002**, *106*, 113.
(19) Stewart, M. P.; Buriak, J. M. *J. Am. Chem. Soc.* **2001**, *123*, 7821.
(20) Wayner, D. D. M.; Wolkow, R. A. *J. Chem. Soc., Perkin Trans. 2* **2002**, 23.
(21) de Smet, L. C. P. M.; Stork, G. A.; Hurenkamp, G. H. F.; Sun, Q.-Y.; Topal, H.; Vronen, P. J. E.; Sieval, A. B.; Wright, A.; Visser, G. M.; Zuilhof, H.; Sudhölter, E. J. R. *J. Am. Chem. Soc.* **2003**, *125*, 13916.
(22) Sun, Q.-Y.; de Smet, L. C. P. M.; van Lagen B.; Wright, A.; Zuilhof, H.; Sudhölter, E. J. R. *Angew. Chem., Int. Ed.* **2004**, *43*, 1352.
(23) Sun, Q.-Y.; de Smet, L. C. P. M.; van Lagen, B.; Giesbers, M.; Thune, P. C.; van Engelenburg, J.; de Wolf, F. A.; Zuilhof, H.; Sudhölter, E. J. R. *J. Am. Chem. Soc.* **2005**, *127*, 2514.
(24) Bateman, J. E.; Eagling, R. D.; Worrall, D. R.; Horrocks, B. R.; Houlton, A. *Angew. Chem., Int. Ed.* **1998**, *37*, 2683.
(25) Boukherroub, R.; Wojtyk, J. T. C.; Wayner, D. D. M.; Lockwood, D. J. *J. Electrochem. Soc.* **2002**, *149*, H59.
(26) Buriak, J. M.; Allen, M. J. *J. Am. Chem. Soc.* **1998**, *120*, 1339.
(27) Stewart, M. P.; Robins, E. G.; Geders, T. W.; Allen, M. J.; Choi, H. C.; Buriak, J. M. *Physica Status Solidi A* **2000**, *182*, 109.
(28) Sieval, A. B.; Opitz, R.; Maas, H. P. A.; Schoeman, M. G.; Meijer, G.; Vergeldt, F. J.; Zuilhof, H.; Sudhölter, E. J. R. *Langmuir* **2000**, *16*, 10359.
(29) Sieval, A. B.; Linke, R.; Zuilhof, H.; Sudhölter, E. J. R. *Adv. Mater.* **2000**, *12*, 1457.
(30) Sailor, M. J.; Lee, E. J. *Adv. Mater.* **1997**, *9*, 783.
(31) Sailor, M. J.; Heinrich, J. L.; Lauerhaas, J. M. *Stud. Surf. Sci. Catal.* **1997**, *103*, 209.
(32) Sieval, A. B.; Demirel, A. L.; Nissink, J. W. M.; Linford, M. R.; van der Maas, J. H.; de Jeu, W. H.; Zuilhof, H.; Sudhölter, E. J. R. *Langmuir* **1998**, *14*, 1759.
(33) Strother, T.; Hamers, R. J.; Smith, L. M. *Nucl. Acid Res.* **2000**, *28*, 3535.
(34) Lin, Z.; Strother, T.; Cai, W.; Cao, X.; Smith, L. M.; Hamers, R. J. *Langmuir* **2002**, *18*, 788.

(35) Strother, T.; Cai, W.; Zhao, X.; Hamers, R. J.; Smith, L. M. *J. Am. Chem. Soc.* **2000**, *122*, 1205.
(36) Juang, A.; Scherman, O. A.; Grubbs, R. H.; Lewis, N. S. *Langmuir* **2001**, *17*, 1321.
(37) Pike, A. R.; Lie, L. H.; Eagling, R. A.; Ryder, L. C.; Patole, S. N.; Connolly, B. A.; Horrocks, B. R.; Houlton, A. *Angew. Chem., Int. Ed.* **2002**, *41*, 615.
(38) Patole, S. N.; Pike, A. R.; Connolly, B. A.; Horrocks, B. R.; Houlton, A. *Langmuir* **2003**, *19*, 5457.
(39) Lie, L. H.; Patole, S. N.; Pike, A. R.; Ryder, L. C.; Connolly, B. A.; Ward, A. D.; Tuite, E. M.; Houlton, A.; Horrocks, B. R. *Faraday Discuss.* **2004**, *125*, 235.
(40) Wang, L.; Reipa, V.; Blasic, J. *Bioconjugate Chem.* **2004**, *15*, 409.
(41) Allongue, P.; de Villeneuve, C. H.; Pinson, J. *Electrochim. Acta* **2000**, *45*, 3241.
(42) Allongue, P.; de Villeneuve, C. H.; Pinson, J.; Ozanam, F.; Chazalviel, J.-N. *Electrochim. Acta* **1998**, *43*, 2791.
(43) Yu, H. Z.; Morin, S.; Wayner, D. D. M.; Allongue, P.; de Villeneuve, C. H. *J. Phys. Chem. B* **2000**, *104*, 11157.
(44) Sieval, A. B.; van den Hout, B.; Zuilhof, H.; Sudhölter, E. J. R. *Langmuir* **2000**, *16*, 2987.
(45) Zhang, L.; Wesley, K.; Jiang, S. *Langmuir* **2001**, *17*, 6275.
(46) Sieval, A. B.; van den Hout, B.; Zuilhof, H.; Sudhölter, E. J. R. *Langmuir* **2001**, *17*, 2172.
(47) Lua, Y. Y.; Niederhauser, T. L.; Matheson, R.; Bristol, C.; Mowat, I. A.; Asplund, M. C.; Linford, M. R. *Langmuir* **2002**, *18*, 4840.
(48) Reboredo, F. A.; Schwegler, E.; Galli, G. *J. Am. Chem. Soc*. **2003**, *125*, 15243.
(49) Kang, J. K.; Musgrave, C. B. *J. Chem. Phys*. **2002**, *116*, 9907.
(50) Kruse, P.; Johnson, E. R.; DiLabio, G. A.; Wolkow, R. A. *Nano Lett*. **2002**, *2*, 807.
(51) Pei, Y.; Ma, J.; Jiang, Y. *Langmuir* **2003**, *19*, 7652.
(52) Ishibashi, T.; Ara, M.; Tada, H.; Onishi, H. *Chem. Phys. Lett.* **2003**, *367*, 376.
(53) Quayum, M. E.; Kondo, T.; Nihonyanagi, S.; Miyamoto, D.; Uosaki, K. *Chem. Lett.* **2002**, 208.
(54) Nihonyanagi, S.; Miyamoto, D.; Idojiri, S.; Uosaki, K. *J. Am. Chem. Soc.* **2004**, *126*, 7034.
(55) Nealey, P. F.; Black, A. J.; Wilbur, J. L.; Whitesides, G. M. In *Molecular Electronics*; Jortner, J., Ratner, M. A., Eds.; Blackwell Science Ltd.: Oxford, U.K., 1997; Ch. 11, pp 343−368.
(56) Lopinski, G. P.; Wayner, D. D. M.; Wolkow, R. A. *Nature* **2000**, *406*, 48.
(57) Cicero, R. L.; Chidsey, C. E. D.; Lopinski, G. P.; Wayner, D. D. M.; Wolkow, R. A. *Langmuir* **2002**, *18*, 305.
(58) Kruse, P.; Johnson, E. R.; DiLabio, G. A.; Wolkow, R. A. *Nano Lett.* **2002**, *2*, 807.
(59) Eves, B. J.; Sun, Q.-Y.; Lopinski, G. P.; Zuilhof, H. *J. Am. Chem. Soc.* **2004**, *126*, 14318.
(60) Cho, J. H.; Oh, D. H.; Kleinman, L. *Phys. Rev. B* **2002**, *65* (8), 081310.
(61) Stewart, M. P.; Buriak, J. M. *Angew. Chem., Int. Ed.* **1998**, *37*, 3257.
(62) Bateman, J. E.; Eagling, R. D.; Houlton, A.; Horrocks, B. R. *J. Phys. Chem. B* **2000**, *104*, 5557.
(63) Asao, N.; Sudo, T.; Yamamoto, Y. *J. Org. Chem.* **1996**, 61, 7654.
(64) *WinFIRST*, v2.10; Analytical Technology Inc.: Madison, WI, 1994.
(65) Burrows, V. A.; Chabal, Y. J.; Higashi, G. S.; Raghavachari, K.; Christman, S. B. *Appl. Phys. Lett.* **1988**, *53*, 998.
(66) Ogata, Y.; Niki, H.; Sakka, T.; Iwasaki, M. *J. Electrochem. Soc.* **1995**, *142*, 195.
(67) Ogata, Y.; Niki, H.; Sakka, T.; Iwasaki, M. *J. Electrochem. Soc.* **1995**, *142*, 1595.
(68) Wave function Inc., Irvine, CA, www.wavefun.com; Schrodinger Inc., Portland, OR, www.schrodinger.com.
(69) GAMESS: Schmidt, M. W.; Baldridge, K. K.; Boatz, J. A.; Elbert, S. T.; Gordon, M. S.; Jensen, J. H.; Koseki, S.; Matsunaga, N.; Nguyen, K. A.; Su, S.; Windus, T. L.; Dupuis, M.; Montgomery, J. A. *J. Comput. Chem.* **1993**, *14*, 1347.
(70) Granovsky, A. A. http://classic.chem.msu.su/gran/gamess/index.html.
(71) Matsumoto, T.; Belogorokhov A. I.; Belogorokhova, L. I.; Masumoto, Y.; Zhukov, E. A. *Nanotechnology* **2000**, *11*, 340.
(72) Matsumoto, T.; Masumoto, Y.; Nakashima, S.; Mimura, H.; Koshida, N. *Appl. Surf. Sci.* **1997**, *113*−*114*, 140.
(73) Matsumoto, T.; Masumoto, Y.; Nakashima, S.; Koshida, N. *Thin Solid Films* **1997**, *297*, 31.
(74) Bateman, J. E.; Eagling, R. D.; Horrocks, B. R.; Houlton, A.; Worrall, D. R. *Chem. Commun.* **1997**, 2275.
(75) *CRC Handbook of Chemistry and Physics*, 75th ed.; Lide, D. R., Ed.; CRC Press: Boca Raton, FL, 1994.
(76) Boukherroub, R.; Morin, S.; Sharpe, P.; Wayner, D. D. M. *Langmuir* **2000,** *16*, 7429.
(77) Buriak, J. M.; Stewart, M. P.; Geders, T. W.; Allen, M. J.; Choi, H. C.; Smith J.; Raftery, D.; Canham, L. T. *J. Am. Chem. Soc.* **1999**, *121*, 11491.
(78) Holland, J. M.; Stewart, M. P.; Allen, M. J.; Buriak, J. M. *J. Solid State Chem.* **1999**, *147*, 251.
(79) Cotton, F. A.; Wilkinson, G. *Advanced Inorganic Chemistry*, 5th ed.; Wiley: New York, 1988; pp 1255−1256.
(80) Boukherroub, R.; Morin, S.; Bensebaa, F.; Wayner, D. D. M. *Langmuir* **1999**, *15*, 3831.
(81) Scott, A. P.; Radom, L. *J. Phys. Chem.* **1996**, *100*, 16502.